Available online at www.sciencedirect.com
ScienceDirect
Journal of Hazardous Materials 153 (2008) 775–783
Journal of Hazardous Materials
www.elsevier.com/locate/jhazmat

Characterization of carbonated tricalcium silicate and its sorption capacity for heavy metals: A micron-scale composite adsorbent of active silicate gel and calcite

Quanyuan Chen [a,*], Colin D. Hills [b], Menghong Yuan [a], Huanhuan Liu [a], Mark Tyrer [c]

[a] School of Environmental Science and Engineering, Donghua University, Shanghai 200051, PR China
[b] School of Science, University of Greenwich, Pembroke, Chatham Maritime, Kent ME4 4TB, UK
[c] Department of Materials, Imperial College of Science, Technology and Medicine, London SW7 4AZ, UK

Received 12 October 2006; received in revised form 6 September 2007; accepted 6 September 2007
Available online 8 September 2007

Abstract

Adsorption-based processes are widely used in the treatment of dilute metal-bearing wastewaters. The development of versatile, low-cost adsorbents is the subject of continuing interest. This paper examines the preparation, characterization and performance of a micro-scale composite adsorbent composed of silica gel (15.9 w/w%), calcium silicate hydrate gel (8.2 w/w%) and calcite (75.9 w/w%), produced by the accelerated carbonation of tricalcium silicate (C_3S, Ca_3SiO_5). The Ca/Si ratio of calcium silicate hydrate gel (C–S–H) was determined at 0.12 (DTA/TG), 0.17 (^{29}Si solid-state MAS/NMR) and 0.18 (SEM/EDS). The metals-retention capacity for selected Cu(II), Pb(II), Zn(II) and Cr(III) was determined by batch and column sorption experiments utilizing nitrate solutions. The effects of metal ion concentration, pH and contact time on binding ability was investigated by kinetic and equilibrium adsorption isotherm studies. The adsorption capacity for Pb(II), Cr(III), Zn(II) and Cu(II) was found to be 94.4 mg/g, 83.0 mg/g, 52.1 mg/g and 31.4 mg/g, respectively. It is concluded that the composite adsorbent has considerable potential for the treatment of industrial wastewater containing heavy metals.

Keywords: Tricalcium silicate (C_3S); Adsorbent; Adsorption capacity; Heavy metal; Wastewater

1. Introduction

Heavy metals are widely used by industry, for example, for electroplating, pigment and paint manufacturing. The metals require removal from industrial effluents before discharge into the environment to mitigate any impact on plant, animal and human receptors. The most common treatment methods for heavy metal-bearing wastewater involve physical and chemical separation techniques. Some conventional methods such as chemical precipitation, ion exchange, and reverse osmosis are not economically feasible or cannot satisfy current discharge standards [1–3]. For example, the minimum solubilities of the different metals usually found in polluted water occur at different pH values and maximum removal efficiencies cannot be achieved at a single pH level [4]. Consequently, the metals precipitation process is very difficult to control and is usually incapable of meeting discharge limits of 0.1–5 mg/L.

Adsorption is very effective for the treatment of wastewater containing low concentration of heavy metals [5–7]. Activated carbon has been the standard adsorbent for the reclamation of municipal and industrial wastewaters, however, it requires regeneration and its adsorption capacity for heavy metals is usually less than 50 mg/g [8–11]. Furthermore, the adsorption density of inorganic species onto activated carbon surfaces varies significantly with pH, in accordance with its acid–base behavior [12].

Cation exchange resins have a much higher adsorption capacity for heavy metals, ranging from 30 mg/g to 90 mg/g, with the maximum 200 mg/g [2,3,13], but the regeneration of spent resin is also problematic and costly. Therefore, recent developments have largely focused on low-cost adsorbents including natural minerals and industrial or agricultural by-products [5], including fly ash [14], granulated furnace slag [15,16], carbonaceous material [17,18], metal oxides [19,20], metal hydroxides [4],

* Corresponding author. Tel.: +86 21 6779 2540; fax: +86 21 6779 2552.
E-mail address: qychen@dhu.edu.cn (Q. Chen).

0304-3894/$ – see front matter © 2007 Elsevier B.V. All rights reserved.
doi:10.1016/j.jhazmat.2007.09.023

bentonite [21,22], zeolites [23,24], lignin, biomass and peanut hulls [25–32]. The adsorption capacity for heavy metals of these materials is commonly in a range of 0.5–30 mg/g [5,7,33], although the capacity of modified bentonite is reported to reach 99 mg/g [34].

The retention of heavy metals on the surface of the mineral calcite was found to the follow the sequence: Cr(III) (217 mg/g) > Zn(II) (185 mg/g) > Cd(II) (16.3 mg/g) according to Garcia-Sanchez and Alvarez-Ayuso [18]. They concluded that the high binding capacity particularly for Cr(III) and Zn(II) was due to metals precipitation rather than adsorption.

Porous silica gel (S–H) and its surface-modified products have been used as adsorbents for the removal of heavy metals and organic matter from industrial or natural discharges [35,36]. Silica gel has usually been ascribed to the condensation of $Si(OH)_4$ into siloxane chains, which branch and cross-link to form a random three-dimensional network. Hong and Glasser reported that calcium silicate hydrate gel (C–S–H) has a very strong sorptivity for various metals [37,38]. Calcium silicate hydrate gel comprises a large and complex 'family' of structures of varying composition [39,40]. Both silica gel and C–S–H gel contain a large number of pores, which range in scale from micro- to macro-size, and these influence sorptivity. An understanding of the relationship between metals sorption capacity and the structure and composition of silica-based sorbents is limited at present.

In order to address this deficiency, the following work investigates the preparation, chemical structure and adsorption properties of an active silica gel comprised of low Ca/Si ratio calcium silicate hydrate gel and calcite. The adsorptive capacity of this composite for Cu(II), Zn(II), Cr(III) and Pb(II) in nitrate solutions are examined. The results of equilibrium adsorption isotherm, kinetic and column adsorption experiments are presented and discussed below.

2. Materials and methods

2.1. Materials

The adsorbent composed of low Ca/Si ratio of calcium silicate hydrate gel and calcite was prepared by carbonating tricalcium silicate (Ca_3SiO_5) or C_3S. The C_3S had been synthesized from a 3:1 molar ratio mixture of $CaCO_3$ and SiO_2 (Aldrich Chemical Company, purity >98%) by grinding to a fine powder in a ceramic ball mill, pelletising and then sintering at 1500 °C for 2 h. After the initial firing, the cycle of grinding, pelletising and sintering was repeated until no free CaO was detected by X-ray diffraction (Fig. 1). The main peaks observed in Fig. 1 are typical of pure C_3S, as described by Taylor [40].

To ensure complete carbonation of C_3S was achieved in an acceptable time frame, a fresh C_3S paste with a solid/liquid ratio of 10:4 was placed in a carbonation chamber supplied with pure CO_2 at constant pressure of 0.3 MPa, a temperature of 17 °C and relative humidity of 50%, maintained by a small bath of saturated NaCl solution. The paste was exposed to CO_2 for 40 min, followed by immediate grinding to <30 μm. This cycle of carbonation/grinding was repeated up to eight times before the material was vacuum-dried and stored in a bag containing carbon dioxide gas.

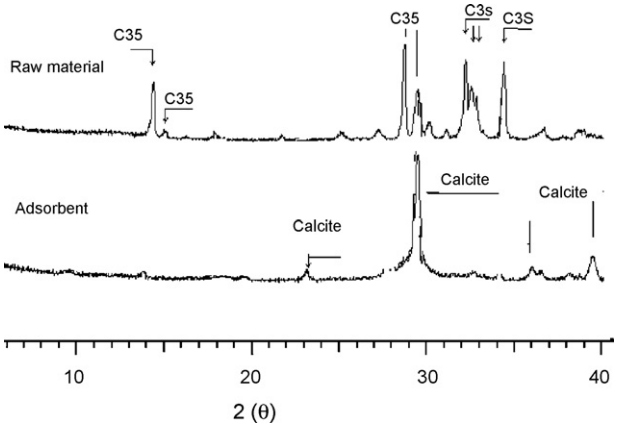

Fig. 1. Diffractograms of raw C_3S and carbonated C_3S.

When ground with an agate mortar and pestle to <10 μm, the surface area of the powdered material was 410 m^2/g (Fig. 2). This high surface area resulted from the large number of gel pores, was measured using a Brunauer–Emmett–Teller (BET) nitrogen sorptometer (Quantasorb surface area analyzer, Model-05). This material was used for batch adsorption experiments, but in column adsorption studies, the grain size was modified to between 0.2 mm and 1 mm to avoid handling difficulties and particle emission to air.

Four single-component metal ion solutions containing chromium, copper, zinc and lead, with different concentrations (100–600 mg/L as heavy metals), were used in this work. The stock solutions were prepared from the nitrate salts: $Cu(NO_3)_2{\cdot}3H_2O$, $Zn(NO_3)_2{\cdot}6H_2O$, $Cr(NO_3)_3{\cdot}9H_2O$ and $Pb(NO_3)_2$ (Aldrich Chemical Company, purity >98%) and deionized water.

2.2. Methods

2.2.1. Characterisation of the composite absorbent

2.2.1.1. X-ray diffraction (XRD). A Siemens D500 diffractometer and Kristalloflex 810 generator (Cu Kα radiation) were used to identify the crystalline phases in the adsorbent. The accelerating voltage was 40 KV and the current was 40 mA. The finely ground samples (<30 μm) were examined between

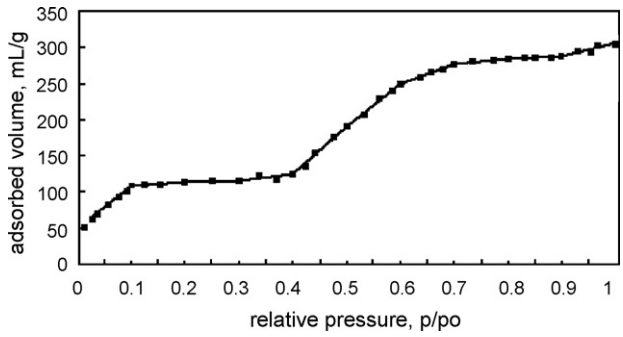

Fig. 2. Nitrogen sorption of the composite adsorbent.

5° and 40° 2θ, at scanning rate of 1° 2θ/min. The diffractograms were obtained with Diffplus and analyzed using Bruker/AXS EVA software and compared with the current version of the international powder data file (ICDD-JCPDS).

2.2.1.2. Thermal analysis (DTA/TG). A Stanton Redcroft STA 780 Simultaneous Thermal Analyzer was used to conduct differential thermal and thermogravimetric analysis (DTA/TG). Samples of 20 mg were ground with an agate mortar and pestle to less <30 μm and packed in a rhodium–platinum crucible (5.8 mm diameter and 4 mm high) and were examined between 30 °C and 1100 °C at a heating rate of 10 °C/min under a flow of nitrogen (40 cm^3/min).

2.2.1.3. Solid-state magic angle spinning/nuclear magnetic resonance (MAS/NMR). ^{29}Si solid-state MAS/NMR spectra were recorded on a Varian Infinity Plus-300 spectrometer equipped with a 7.1 T magnet, at the resonance frequency for ^{29}Si, which is 59.49 MHz. All samples were spun at a rate of 6 KHz to improve signal resolution. NMR experiments were operated at relaxation $T_1 \gg 30$ s with a relaxation delay of 10 s. ^{29}Si chemical shifts were reported relative to tetramethysilane (TMS).

2.2.1.4. Scanning electron microscopy and energy dispersive X-ray spectroscopy (SEM/EDS). Morphological studies and microanalyses were conducted using a JEOL JSM-640 SEM equipped with an energy dispersive X-ray spectrometer (LINK ANINCA, LINK ISIS 300) at an accelerating voltage of 15 kV. To provide qualitative and semi-quantitative information on the elemental composition of the adsorbent matrix, 90 separate analyses were used. The incident beam was intentionally centered in the middle of particle clusters to minimize the influence of the different phases on the X-rays generated.

2.2.2. Adsorption capacity studies

Equilibrium adsorption isotherm studies were performed to determine the relationship between the capacity of the adsorbent for metal ions and equilibrium metal ion concentrations. In the batch sorption studies, 200 mL of each metal nitrate solution (100–600 mg/L heavy metal) was shaken (30 r/min) with 1 g of the adsorbent in 250 mL screw-top plastic bottles at an ambient temperature of 17 °C. After a contact time of 60 min (unless otherwise stated below), the solutions were centrifuged at 3500 rpm for 15 min and filtered through a 0.45 μm membrane filter. The filtrates were analyzed in duplicate for using a dual view inductively coupled plasma-atomic emission spectroscopy, ICP-AES (Perkin-Elmer). The adsorbent loading was determined by the difference in the ion content before and after the adsorption equilibrium had been established. The results presented are simple means with a relative deviation of less than 5%.

2.2.3. Column adsorption assays

Continuous flow adsorption studies were carried out in a perspex column packed with 75 g of the adsorbent with particle size of ranging in 0.2–1 mm. The initial solution concentration was 50 mg/L, and was passed through the column (diameter: 2 cm, height: 15 cm, BV 32 mL) at a flow rate of 5 mL/min using a peristaltic pump. Effluent samples were collected from the column end at regular time intervals for analysis by ICP-AES.

2.2.4. Leaching

The spent materials generated from the continuous flow adsorption studies were leach tested using the DIN 38414-S4 leaching procedure. Twenty grams of each spent adsorbent (<30 μm) was placed in 200 mL of distilled water (L/S 10) in a plastic bottle and rotated at 30 rpm for 24 h at an ambient temperature of 17 °C. The leachates were then filtered through a 0.45 μm membrane filter prior to analysis by ICP-AES.

3. Results and discussion

3.1. Characteristics of the composite adsorbent

As shown in Fig. 1, after carbonation the reflections observed for raw C_3S were absent, indicating that carbonation was complete. Silica gel (S–H) and calcium silicate hydrate gel (C–S–H) are amorphous and cannot be detected by XRD, whereas reflections for calcite were detected at 23°, 29.5°, 36.1° and 39.5° 2θ. Thus, the material prepared from carbonated C_3S consisted of silica gel, calcium silicate hydrate gel and calcite according to the following reaction:

$$C_3S + H_2O + CO_2 \rightarrow CaCO_3 + \text{C–S–H} + \text{silica gel (S–H)} \quad (1)$$

Based on the DTA/TG analysis (Fig. 3), the calcium carbonate content in the composite adsorbent was determined from the following equation:

$$C\underline{C}\,(\%) = \frac{WL_{C\underline{C}}(\%) \times MW_{C\underline{C}}}{MW_{\underline{C}}} \quad (2)$$

where $C\underline{C}$ (%) is the content of $CaCO_3$, $WL_{C\underline{C}}$ (%) the weight loss during the decomposition of calcium carbonate at 600–850 °C, $MW_{\underline{C}}$ and $MW_{C\underline{C}}$ are the molar weight of carbon dioxide and calcium carbonate. Table 1 presents the thermal analyses and the estimated content of calcium carbonate, was 75.9 w/w% which is very close to the theoretical content of 77.01 w/w% calculated from the chemical compositions of the

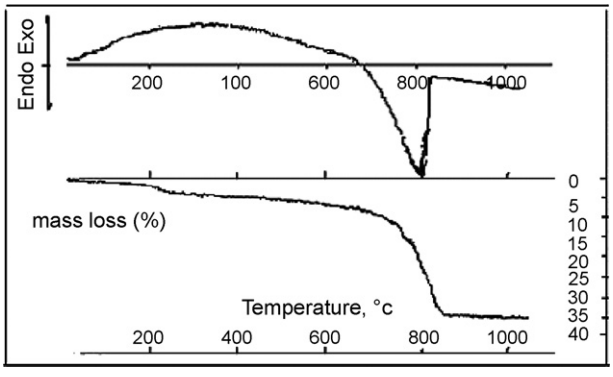

Fig. 3. DTA/TG thermograms for carbonated C_3S powder.

Table 1
Thermal analysis results of carbonated C_3S

Weight loss (%)	
20–250 °C	3.1
250–600 °C	4.2
600–850 °C	33.4
Composition (%)	
H_2O	7.3
$CaCO_3$	75.9
C–S–H plus SiO_2 gel	24.1
Ca/Si in gel	0.12

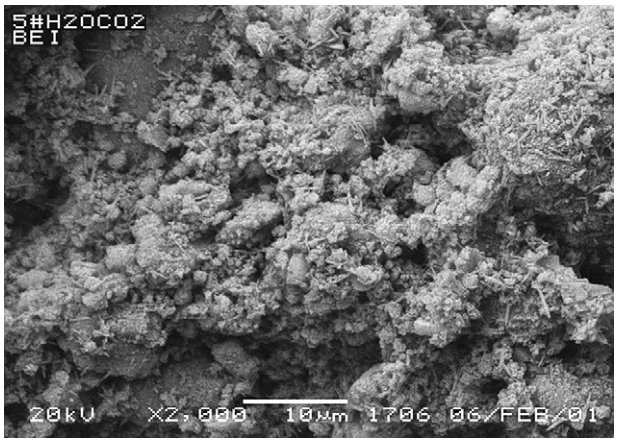

Fig. 4. Electron micrograph of the composite adsorbent (scale bar is 10 μm).

raw material (C_3S). C–S–H gel and silica gel comprised approximately 24.1% of the carbonated products by mass and according to the thermal analysis. The estimated average Ca/Si ratio of silicate gel was 0.12, which was calculated by the following equation:

$$\text{Ca/Si} = \frac{\text{total Ca} - \text{Ca in calcium carbonate}}{\text{total Si}} \quad (3)$$

An electron micrograph showing a fracture surface of carbonated C_3S is presented in Fig. 4. Silica gel and C–S–H gel appeared as porous fibers whereas calcite appeared as equant grains. The porous silica gel aggregates were around 300 nm to 3 μm in size, whereas for calcite, grains were typically <5 μm. The composition of C–S–H gel obtained from the EDS microanalysis of carbonated C_3S paste, are shown in Table 2. The average Ca/Si ratio of C–S–H gel taken from 90 spot analyses was 0.18. This is consistent with the result obtained from DTA/TG. It is worth noting that very low Ca/Si ratio C–S–H gel, with a Ca/Si of 0.07 was observed. Variations in Ca/Si of this magnitude would ultimately influence the metals adsorption

Table 2
EDS microanalysis results for C–S–H in carbonated C_3S paste

Analysis spots	SiO_2 (%)	CaO (%)	Ca/Si
15 spots	94.01	4.35	0.07
63 spots	77.19	13.36	0.19
13 spots	73.45	16.88	0.25
The average value of 90 spots	79.43	12.38	0.18

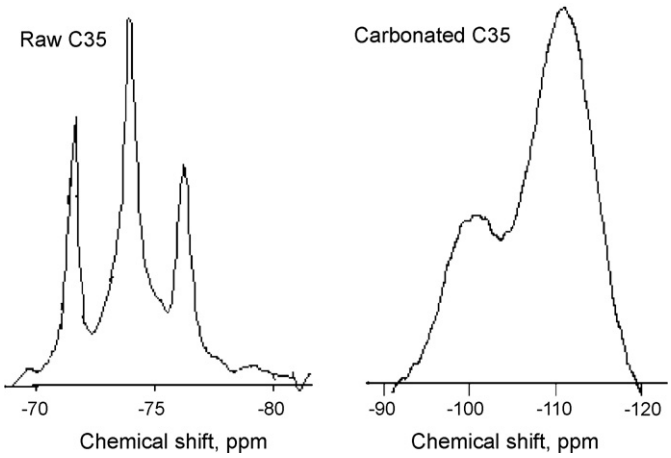

Fig. 5. ^{29}Si NMR spectra of raw and carbonated C_3S.

capacity of C–S–H via cation exchange capacity and physical and chemical adsorption characteristics [37,39,41].

Solid-state magic angle spinning/nuclear magnetic resonance (MAS/NMR) was employed to study the chemical structure of silicate phases of the composite adsorbent. ^{29}Si NMR spectra from raw C_3S and carbonated C_3S are presented in Fig. 5. As a general rule, the distribution of silicate tetrahedra with varying numbers (n) of bridging oxygen are commonly described as Q^n species, which can be estimated from the peak intensities obtained. In this study, three peaks from the raw C_3S were observed at −71.9 ppm, −74.5 ppm and −76.2 ppm, and were characteristic for the mono-silicate group (Q^0). The three resonance peaks in raw C_3S reflect the differences in silicon chemical environments, that is, the differences in bond angle and bond length of (–O–Si–O–Ca–) groups and the presence of polymorphs of C_3S.

The crystal structure of C_3S is complex, as it depends on processing conditions, cooling conditions and the raw materials used, including the trace impurities present, which can deform a crystalline structure [40]. Lippmaa et al. reported that the spectra of C_3S consisted at least six narrow lines in the range from −69.3 ppm to −74.5 ppm, with the line at −73.7 ppm being the most intense one [42,43].

As shown in Fig. 5, after carbonation, Q^0 species were absent, indicating that the carbonation of C_3S was complete and this was in accordance with the XRD examination. The silicate end (Q^1) and middle groups (Q^2) were not detected and the framework sites were the dominant species over branching sites. The proportion of Q^3 and Q^4 species were 33.96% and 66.04%, respectively. Thus the carbonation of C_3S resulted in the polymerization of silicates from isolated tetrahedra to branching sites (a very low Ca/Si ratio of C–S–H gel) and three-dimensional frameworks (silica gel, S–H). These polymerized silicate phases are summarized in Table 3. The connectivity (C) and Ca/Si ratio for the silicate phases in carbonated C_3S were determined by the following equations [44–46]:

$$C = \frac{Q^1 + 2Q^2 + 3Q^3 + 4Q^4}{Q^1 + Q^2 + Q^3 + Q^4} = 3.66 \quad (4)$$

Table 3
Silicon species from raw and carbonated C_3S based on the ^{29}Si NMR spectra (%)

Sample	Q^0 (ppm)			Q^3 (ppm)	Q^4 (ppm)
	−71.9	−74.5	−76.2	−100	−110
Raw C_3S (%)	30.77	42.31	26.92	0	0
Carbonated C_3S (%)	0	0	0	33.96	66.04

$$\mathrm{Ca/Si} = 2Q^0 + 1.5Q^1 + Q^2 + 0.3Q^3 = 0.17 \quad (5)$$

where Q^0, Q^1, Q^2, Q^3 and Q^4 are the percentages determined for the respective species. Note that the Ca/Si ratio of C–S–H gel in the carbonated C_3S pastes was 0.17, which was in agreement with the results obtained from both the DTA/TG and SEM/EDS analyses.

It is therefore estimated that the carbonated C_3S powder comprised silica gel (15.9%) and C–S–H gel (8.2%), assuming that Q^3 dominates C–S–H and Q^4 for S–H, as shown as Eqs. (6) and (7).

Q^3 species:

$$m\mathrm{C_3S} + q\mathrm{H_2O} + \mathrm{CO_2} \rightarrow y\mathrm{CaCO_3} + \mathrm{Ca}_x\mathrm{H}_{(m-2x)}(\mathrm{SiO_{2.5}})_m \cdot z\mathrm{Ca[(OH)_2, CO_3]} \cdot n\mathrm{H_2O} \quad (6)$$

where m should be a large number; $n > 0$; $q > 0$; $z = 0, 1, 2, 3$, etc.

Q^4 species:

$$m\mathrm{C_3S} + q\mathrm{H_2O} + \mathrm{CO_2} \rightarrow y\mathrm{CaCO_3} + (\mathrm{SiO_2})_m \cdot n\mathrm{H_2O} \quad (7)$$

where m should be a large number; and $n > 0$; $q > 0$.

3.2. Adsorption studies

3.2.1. pH variation of suspensions and adsorption kinetics

For simplicity, the carbonated C_3S powder, containing silica gel and calcite is referred to as the 'composite adsorbent' below. Heavy metal nitrate solutions with a concentration of 300 mg/L (as heavy metal ions) were placed in sealed containers and the composite adsorbent was added at a solid/liquid ratio of 1:200. The suspension was agitated and the resultant pH values were measured (Philips DW9418 pH meter) at regular time intervals (Fig. 6). The initial pH of the suspensions containing Cu(II), Pb(II), Zn(II) and Cr(III) ranged from 6.0 to 6.5. The suspension pH values rose over time, due to the decalcification of C–S–H gel and after 240 h, reached pH 7.0–7.5. The hydrolysis of the heavy metal cations in the nitrate resulted in a lower solution pH in comparison to the control suspension (pH 8.5) containing de-ionised water and composite adsorbent.

The kinetics of heavy metals removal by the composite adsorbent is shown in Fig. 7. In this experiment, the L/S ratio was 1000:1 (1 g/L) and employed 300 mg/L solutions (metal). Adsorption increased with contact time and an equilibrium was established when the concentration of metal in a bulk solution was in dynamic balance with that on the surfaces of the composite adsorbent. Equilibrium conditions were established within 60 min for all systems investigated.

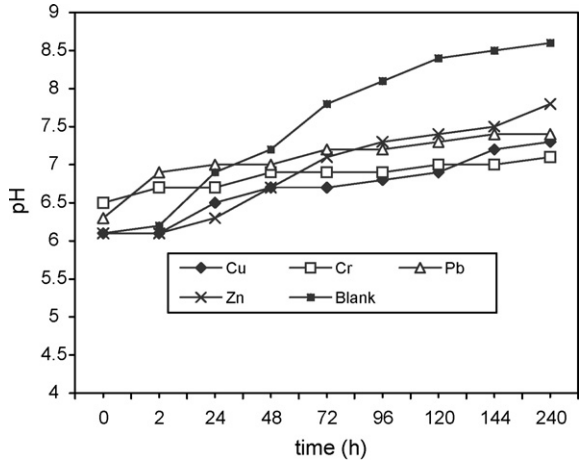

Fig. 6. Change in suspension pH with time.

3.2.2. Sorption isotherms

The Langmuir and Freundlich equations are used to describe adsorption isotherms under constant temperature conditions. Langmuir isotherm constants may be obtained from the plot of $1/q_e$ against $1/C_e$:

$$\frac{1}{q_e} = \frac{1}{q_{max}} + \frac{1}{q_{max} b C_e} \quad (8)$$

where q_e (mg/g) and C_e (mg/L) are the amount of adsorbed metal ions per unit mass of adsorbent and the un-adsorbed metal ion concentration in solution at equilibrium, respectively. q_{max} (mg/g) is adsorption capacity and b is a constant related to the affinity of the binding sites (L/mg).

Similarly, the Freundlich constants may be obtained from the plot of $\lg q_e$ against $\lg C_e$:

$$\lg q_e = \frac{1}{n} \lg C_e + \lg K_F \quad (9)$$

where C_e is the equilibrium concentration of the metal ions (mg/L); q_e the amount of metals adsorbed per unit mass of adsorbent (mg/g); K_F (mg/g (L/mg)$^{1/n}$) and n (dimensionless) signifies the adsorption capacity and adsorption intensity respectively. In other words, n gives an indication of how favorable the adsorption process is; K_F can be defined as the adsorption

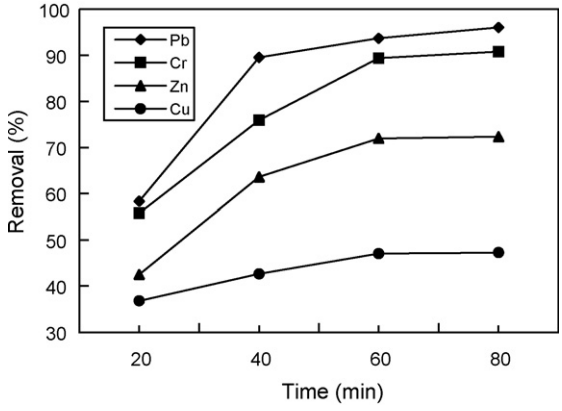

Fig. 7. Adsorption kinetics of heavy metals on the composite adsorbent.

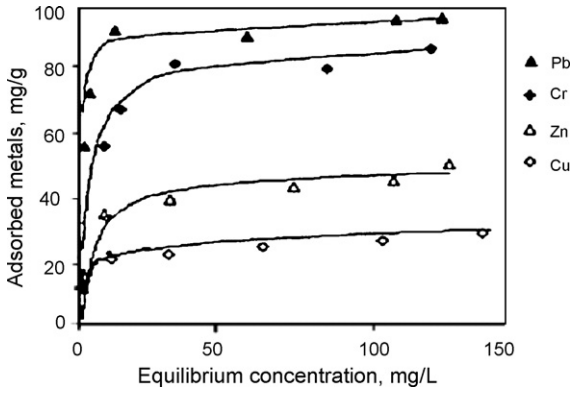

Fig. 8. Sorption isotherms for Cu(II), Pb(II), Zn(II) and Cr(III).

or distribution coefficient and represents the quantity of metals adsorbed onto adsorbent at the equilibrium concentration. The Freundlich equation describes adsorption onto a heterogeneous surface. The slope of *1/n* ranging between 0 and 1 is a measure of surface heterogeneity, with the surface becoming more heterogeneous as its value gets closer to zero. 1/*n* above one is indicative of cooperative adsorption.

The Langmir–Freundlich isotherm is the combination of both equation, and is an empirical model that incorporates the features of both isotherms as given in the following equation:

$$q_e = \frac{q_{LF} K_{LF} (C_e)^{1/n}}{1 + q_{LF} K_{LF} (C_e)^{1/n}} \quad (10)$$

where K_{LF} ((L/mg)$^{1/n}$), q_{LF} (mg/g) and n (dimensionless) are the three adjustable empirical parameters (modified Langmuir constants).

According to the adsorption procedure described in the experimental section, the dependency of the adsorbed amounts of metals on their equilibrium concentrations in the solution was measured after a contact time of 60 min (Fig. 8). The linear fitting curves obtained from the sorption isotherms of Cu(II), Pb(II), Zn(II) and Cr (III) onto the composite adsorbent are given in Table 4. The experimental data were further fitted to the Langmuir–Freundlich isotherm equation. The Langmuir–Freundlich isotherm constants were determined by minimizing the error in the experimental data by using the Langmuir EXT model in software Origin 6.0 using the Langmuir constants as the initial values. The sorption constants for Cu(II), Pb(II), Zn(II) and Cr(III) on the composite adsorbent and regression coefficients (R^2) are given in Table 5. From the results shown in Tables 4 and 5, it can be see that 1/*n* ranges between 0.07 and 0.18 for the Freundlich isotherms, indicating that the surface heterogeneity of the composite adsorbent is very significant, indicating that all the 'mineral' components (silica gel, calcium silicate hydrate gel and calcite) take part in the adsorption reaction. From the regression coefficient values given in Table 5, the very low R^2 value of 0.47 shows that it is inappropriate to use the Freundlich isotherm to explain the sorption of Pb(II) ions whereas, the high R^2 value of 0.98 for Pb(II) or Zn(II) shows that it is appropriate to use the Langmuir isotherm. It is obvious that the regression coefficients of fitting to the Langmuir–Freundlich equation are higher than the individual Langmuir and Freundlich equations, demonstrating the suitability of the combined equation.

From the Langmuir parameter, q_{max} (mg/g), the adsorption capacity of the composite adsorbent at saturation was 83.0 mg/g, 94.4 mg/g, 52.1 mg/g and 31.4 mg/g for Cr(III), Pb(II), Zn(II) and Cu(II), respectively. The regression analysis using the Freundlich and the Langmuir–Freundlich isotherms also indicated that the metals adsorption capacity and intensity were in the sequence: Pb(II) > Cr(III) > Zn(II) > Cu(II). The high metals sorption capacity obtained can be compared to other typical

Table 4
Adsorption isotherms for the metals examined

Metal	Langmir isotherm	Freundlich isotherm	Langmir-Freundlich isotherm
Cu	$1/q_e = 0.142/C_e + 0.032$	$\lg q_e = 0.07 \lg C_e + 1.33$	$q = \frac{27.77 \times 0.001\, C_e^4}{1+27.77 \times 0.001\, C_e^4}$
Zn	$1/q_e = 0.203/C_e + 0.019$	$\lg q_e = 0.17 \lg C_e + 1.34$	$q = \frac{41.28 \times 0.01\, C_e^{2.82}}{1+41.28 \times 0.01\, C_e^{2.82}}$
Cr	$1/q_e = 0.049/C_e + 0.012$	$\lg q_e = 0.18 \lg C_e + 1.56$	$q = \frac{78.14 \times 0.16\, C_e^{1.47}}{1+78.14 \times 0.16\, C_e^{1.47}}$
Pb	$1/q_e = 0.012/C_e + 0.011$	$\lg q_e = 011 \lg C_e + 1.76$	$q = \frac{97.82 \times 0.03\, C_e^{1.81}}{1+97.82 \times 0.03\, C_e^{1.81}}$

Table 5
Adsorption constants for the metals examined

Ion	Langmuir isotherm			Freundlich isotherm			Langmuir–Freundlich isotherm			
	q_{max}	b	R^2	n	K_F	R^2	q_{LF}	K_{LF}	n	R^2
Cu	31.35	0.23	0.84	14.03	21.38	0.79	27.77	0.001	0.25	0.95
Zn	52.08	0.10	0.98	5.96	21.67	0.92	41.28	0.011	0.36	0.97
Cr	82.99	0.25	0.88	5.69	36.04	0.71	78.14	0.160	0.57	0.93
Pb	94.43	0.09	0.98	8.88	57.56	0.47	97.82	0.030	0.55	0.95

Note: q_{max} in (mg/g), b in (L/mg), K_F in (mg/g(L/mg)$^{1/n}$), K_{LF} in (L$^{1/n}$/mg$^{1/n}$), q_{LF} in (mg/g).

Table 6
Adsorption capacities for heavy metals

Adsorbent	q_{max} (mg/g)	References
Natural zeolite	Cu 6.74	[23]
Slag	Pb 32.26–95.24, Cu 26.21–88.50	[15,16]
Activated carbon	Cr(VI) 20	[11]
Calcite	Cr 217, Zn 185, Cd 16.3	[18]
Synthetic tobermotite	Cd 2.0, Pb 1.99, Zn 1.94	[50]
Activated montmorillonite	Cd 33.2, Co 29.7, Cu 32.3, Pb 34.0, Ni 29.5	[51]
Peanut	Pb 30, Cu 10, Cd 6, Zn 10	[33]
Resin	Pb 200, Cu 85, Cd 50, Zn 90	[13]
Carbon nanotube	Zn 13.04	[52]

adsorbents in Table 6 and can be attributed to the large surface area and high sorption activity of silica gel and C–S–H gel. In addition, calcite can bind heavy metals by chemical adsorption [17,18,47], indicating that all the mineral components behave as a positive synergistic action.

It is now generally accepted that the surface of silicon atoms tend to have a complete tetrahedral configuration and that in an aqueous medium their free valence becomes saturated with hydroxyl ions, forming silanol groups [16,37,38,46,48,49]. In the presence of trivalent or divalent heavy metal ions (M^{3+} or M^{2+}) the chemical adsorption mechanisms of heavy metals in solution on the surfaces of silica gel and calcite can be illustrated as follows:

$$(SiO_2)_m{\cdot}nH_2O/SiO_2H_2{}^{++} + M^{2+} \rightarrow (SiO_2)_m{\cdot}nH_2O/SiO_2M^{++} + 2H^+ \quad \text{(at low pH)} \quad (11)$$

$$(SiO_2)_m{\cdot}nH_2O/SiOH + MOH^+ \rightarrow (SiO_2)_m{\cdot}nH_2O/SiOM^+ + H_2O \quad \text{(at mediate pH)} \quad (12)$$

$$(SiO_2)_m{\cdot}nH_2O/SiO^- + MOH_x{}^{(x-2)-} \rightarrow (SiO_2)_m{\cdot}nH_2O/SiOM(OH)_{x-1}{}^{(x-3)-} + H_2O \quad \text{(at high pH)} \quad (13)$$

$$CaCO_3/H^+ + M^{2+} \rightarrow CaCO_3/M^{2+} + H^+ \quad \text{(at low pH)} \quad (14)$$

$$CaCO_3/OCa + MOH^+ \rightarrow CaCO_3/M^- + Ca^{2+} + H_2O \quad \text{(at mediate pH)} \quad (15)$$

$$CaCO_3/OH^- + MOH_x{}^{(x-2)-} \rightarrow CaCO_3/OM(OH)_{x-1}{}^{(x-3)-} + H_2O \quad \text{(at high pH)} \quad (16)$$

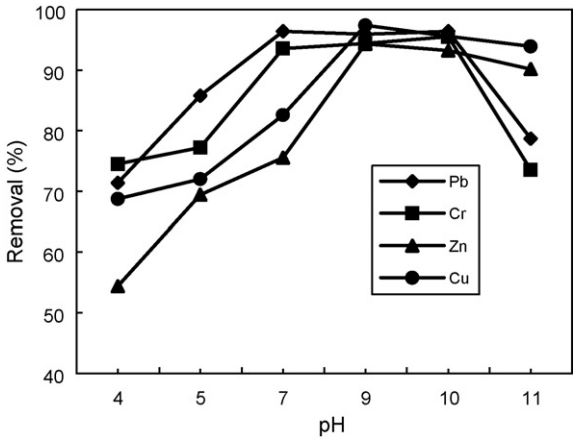

Fig. 9. Influence of pH on heavy metal adsorption.

The mechanism governing heavy metal uptake by C–S–H gel (Q^3 species) is more complex because of its thermodynamic meta-stability, giving rise to the adsorption characteristics of both silica gel and calcium carbonate. Additionally, the incongruent dissolution of calcium cations in C–S–H gel would play an important role in the removal of heavy metals by, for example, causing pH to rise, the co-precipitation of double hydroxides and enhancement of adsorption due to variation in the surface charge.

3.2.3. *Effects of pH on adsorption*

By using CO_2 and NaOH to regulate solution pH, the dissolution of calcite (at low pH) and the influence of initial pH on heavy metals removal, was investigated. The initial metals solution concentration was 100 mg/L (w/w metal), the adsorbent dose was 1 g/L and the contact time was 60 min. The pH values for the 100% CO_2 saturated adsorbent suspensions were pH 4 after 30 min of contacting time, but pH 5 after 10 min. As seen in Fig. 9, the metals uptake was quite high with the optimal pH values for the metal sorption being 8–10, due to metal speciation, silica gel surface charge, the presence of calcite, and chemical binding forces on the substrate surface. It can be observed that metals uptake by the composite adsorbent will decrease with increasing and decreasing pH, due to increasing surface charges at these pH's.

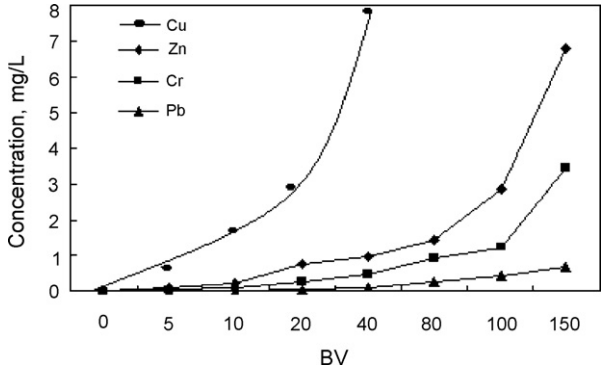

Fig. 10. Breakthrough curves for heavy metals solutions filtered through the adsorbent bed.

Table 7
Metals concentration in leachates from the spent composite adsorbent

Element	Ca	Si	Cu	Zn	Pb	Cr
Concentration (mg/L)	93.71	29.49	0.09	0.21	0.17	0.13
Leaching criteria (mg/L)*	–	–	2–100	2–100	0.4–5	0.1–<15

* Note: Chinese standard, HJ/T299-2007, GB175085.3-2007.

3.2.4. Continuous flow adsorption

The data obtained from the percolation of metal solutions through the composite adsorbent bed are given in Fig. 10. The metal concentrations surpassed the limits (0.1–5 mg/L) between 30 and 80 bed volumes (BV) of percolating solutions. In keeping with the results obtained in the equilibrium and kinetic studies, the composite adsorbent showed the best capacity for Pb(II) ion adsorption. It was possible to treat 150 BV, obtaining an effluent concentration of $\leq$1 mg/L, indicating that the column is suitable to treat heavy metal-bearing solutions.

3.3. Leaching studies

Calcite is dissolved from the composite adsorbent in contact with acid media. The leaching of the spent adsorbent in the column experiments used the DIN 38414 leaching procedure, previously described, at a S/L ratio of 1:20. The filtrates were centrifuged and filtered and after measuring the pH, and the leachate was acidified for analysis by ICP-AES. The results indicate that the heavy metal loaded adsorbent exhibited low leaching of heavy metals and thus, may have a low environmental impact (Table 7).

4. Conclusions

The main objective of the present work was to investigate the binding capacity of a cost effective adsorbent with potential for the removal of metal ions from aqueous waste streams. The main research findings are summarized as follows.

The fully carbonated C_3S consisted of calcite (75.9%), silica gel (15.9%) and low Ca/Si ratio C–S–H gel (8.2%). The particle size was commonly in the range, 300 nm to 5 μm and was composed of active silica gel, C–S–H gel and calcite. The material had a high sorptive capacity for heavy metal ions in aqueous solution.

Examination of the adsorbent retention capacity for heavy metals indicated that: (1) the binding capacities were 94.4 mg/g Pb(II), 83.0 mg/g Cr(III), 52.1 mg/g Zn(II) and 31.4 mg/g Cu(II), respectively; (2) equilibrium conditions were established within 60 min; and (3) the optimal pH range for the sorption of the metal ions was pH 6–9.5.

The composite adsorbent appears to be suitable for the removal of heavy metal ions from wastewater over a wide range of concentrations and pH conditions. However, the effects of the particle size on the adsorption of heavy metals and how the sorbent might best be deployed in practice requires further work.

References

[1] J. Horacek, L. Soukupova, M. Puncochar, et al., Purification of wastewaters containing low concentrations of heavy metals, J. Hazard. Mater. 37 (1994) 69–76.
[2] O. Tuenay, Developments in the application of chemical technologies to wastewater treatment, Water Sci. Technol. 48 (2003) 43–52.
[3] T.A. Kurniawan, G.Y.S. Chan, W.H. Lo, S. Babel, Physico-chemical treatment techniques for wastewater laden with heavy metals, Chem. Eng. J. 118 (2006) 83–98.
[4] K.A. Baltpurvins, R.C. Burns, G.A. Lawrance, Use of the solubility domain approach for the modeling of the hydroxide precipitation of heavy metals from wastewater, Environ. Sci. Technol. 30 (1996) 1493–1499.
[5] S. Babel, T.A. Kurniawan, Low-cost adsorbents for heavy metals uptake from contaminated water: a review, J. Hazard. Mater. 97 (2003) 219–243.
[6] M.J.S. Yabe, E. Oliveira, Heavy metals removal in industrial effluents by sequential adsorbent treatment, Adv. Environ. Res. 7 (2003) 263–272.
[7] Y. Wang, S. Lin, R. Juang, Removal of heavy metal ions from aqueous solutions using various low-cost adsorbents, J. Hazard. Mater. 102 (2003) 291–302.
[8] V. Rajeshwarisivaraj, Subburam, Activated parthenium carbon as an adsorbent for the removal of dyes and heavy metal ions from aqueous solution, Bioresour. Technol. 85 (2002) 205–206.
[9] Y. Kikuchi, Q. Qian, M. Machida, H. Tatsumoto, Effect of ZnO loading to activated carbon on Pb(II) adsorption from aqueous solution, Carbon 44 (2006) 195–202.
[10] C. Moon, J. Lee, Use of curdlan and activated carbon composed adsorbents for heavy metal removal, Process Biochem. 40 (2005) 1279–1283.
[11] S. Babel, T.A. Kurniawan, Cr(VI) removal from synthetic wastewater using coconut shell charcoal and commercially activated carbon modified with oxidising agents and/or chitosan, Chemosphere 54 (2004) 951–967.
[12] F. Pagnanelli, F. Vegliò, L. Toro, Modelling of the acid–base properties of natural and synthetic adsorbent materials used for heavy metal removal from aqueous solutions, Chemosphere 54 (2004) 905–915.
[13] A. Demirbaş, E. Pehlivan, F. Gode, T. Altun, G. Arslan, Adsorption of Cu(II), Zn(II), Ni(II), Pb(II), and Cd(II), from aqueous solution on Amberlite IR-120 synthetic resin, J. Colloid Interface Sci. 282 (2005) 20–25.
[14] K.S. Hui, C.Y.H. Chao, S.C. Kot, Removal of mixed heavy metal ions in wastewater by zeolite 4A and residual products from recycled coal fly ash, J. Hazard. Mater. 127 (2005) 89–101.
[15] S.V. Dimitrova, D.R. Mehandgiev, Lead removal from aqueous solution by granulated blast furnace slag, Water Res. 32 (1998) 3289–3292.
[16] D. Feng, J.S.J. van Deventer, C. Aldrich, Removal of pollutants from acid mine wastewater using metallurgical by-product slags, Sep. Purif. Technol. 40 (2004) 61–67.
[17] J.M. Zachara, C.E. Cowan, C.T. Resch, Sorption of divalent metals on calcite, Geochim. Cosmochim. Acta 55 (1991) 1549–1562.
[18] A. Garcia-Sanchez, E. Alvarez-Ayuso, Sorption of Zn, Cd and Cr on calcite. Application to purification of industrial wastewaters, Miner. Eng. 15 (2002) 539–547.
[19] T.K. Sen, S.P. Mahajan, K.C. Khilar, Adsorption of Cu^{2+} and Ni^{2+} on iron oxide and kaolin and its importance on Ni^{2+} transport in porous media, Colloids Surf. A: Physicochem. Eng. Aspects 211 (2002) 91–102.
[20] S. Kundu, A.K. Gupta, Adsorption characteristics of As(III) from aqueous solution on iron oxide coated cement (IOCC), J. Hazard. Mater. 142 (2007) 97–104.

[21] O. Lacin, B. Bayrak, O. Korkut, E. Sayan, Modeling of adsorption and ultrasonic desorption of cadmium(II) and zinc(II) on local bentonite, J. Colloid Interface Sci. 292 (2005) 330–335.
[22] K.G. Bhattacharyya, S.S. Gupta, Pb(II) uptake by kaolinite and montmorillonite in aqueous medium: influence of acid activation of the clays, Colloids Surf. A: Physicochem. Eng. Aspects 277 (2006) 191–200.
[23] M.I. Panayotova, Kinetics and thermodynamics of copper ions removal from wastewater by use of zeolite, Waste Manag. 21 (2001) 671–676.
[24] E. Erdem, N. Karapinar, R. Donat, The removal of heavy metal cations by natural zeolites, J. Colloid Interface Sci. 280 (2004) 309–314.
[25] S.J. Allen, P.A. Brown, L.J. Whitten, M.A. Murray, O.P. Duggan, The adsorption of pollutants by peat, lignite and activated chars, J. Chem. Technol. Biotechnol. 68 (1997) 442–452.
[26] M.S. Azab, P.J. Peterson, The removal of cadmium from water by the use of biological sorbents, Water Sci. Technol. 21 (1989) 1705–1706.
[27] F.E. Okieimen, E.U. Okundia, D.E. Ogbeifun, Sorption of cadmium and lead ions on modified groundnut husks, J. Chem. Technol. Biotechnol. 51 (1991) 97–103.
[28] K. Perisamy, C. Namasivayam, Removal of nickel (II) from aqueous solution and nickel plating industry wastewater using agricultural waste: peanut hulls, Waste Manag. 15 (1995) 66–68.
[29] M.A.M. Khraisheh, Y.S. Al-degs, W.A.M. Mcminn, Remediation of wastewater containing heavy metals using raw and modified diatomite, Chem. Eng. J. 99 (2004) 177–184.
[30] A. Aklil, M. Mouflih, S. Sebti, Removal of heavy metal ions from water by using calcined phosphate as a new adsorbent, J. Hazard. Mater. 112 (2004) 183–190.
[31] S. Larous, A.-H. Meniai, M.B. Lehocine, Experimental study of the removal of copper from aqueous solutions by adsorption using sawdust, Desalination 185 (2005) 483–490.
[32] S. Pradhan, S.S. Shukla, K.L. Dorris, Removal of nickel from aqueous solutions using crab shells, J. Hazard. Mater. 125 (2005) 201–204.
[33] P. Brown, I.A. Jefcoat, D. Parrish, S. Gill, E. Graham, Evaluation of the adsorptive capacity of peanut hull pellets for heavy metals in solution, Adv. Environ. Res. 4 (2000) 19–29.
[34] F. Ayari, E. Srasra, M. Trabelsi-Ayadi, Characterization of bentonitic clays and their use as adsorbent, Desalination 185 (2005) 391–397.
[35] L. Bois, A. Bonhommé, A. Ribes, et al., Functionalized silica for heavy metal ions adsorption, Colloids Surf. A: Physicochem. Eng. Aspects 221 (2003) 221–230.
[36] R.S.A. Machado Jr., M. Fonseca, L.N.H. Arakaki, et al., Silica gel containing sulfur, nitrogen and oxygen as adsorbent centers on surface for removing copper from aqueous/ethanolic solutions, Talanta 63 (2004) 317–322.
[37] S.Y. Hong, F.P. Glasser, Alkali binding in cement pastes. Part I. The C–S–H phase, Cem. Concr. Res. 29 (1999) 1893–1903.
[38] S.Y. Hong, F.P. Glasser, Alkali sorption by C–S–H and C–A–S–H gels. Part II. Role of alumina, Cem. Concr. Res. 32 (2002) l101–l111.
[39] H.F.W. Taylor, Nanostructure of C–S–H: current status, Adv. Cem. Based Mater. 1 (1993) 38–46.
[40] H.F.W. Taylor, Cement Chemistry, Thomas Telford Publishing, London, 1997.
[41] R.K. Iler, The Chemistry of Silica, A Wiley-Interscience Publication, John Wiley & Sons, New York, 1982.
[42] E. Lippmaa, M. Magi, A. Samoson, G. Engelhardt, A.R.G. Grimmer, Structural studies of silicates by solid-state high resolution ^{29}Si NMR, J. Am. Chem. Soc. 102 (1980) 4889–4893.
[43] E. Lippmaa, M. Magi, M. Tarmak, A high resolution ^{29}Si NMR study of the hydration of tricalcium silicate, Cem. Concr. Res. 12 (1982) 597–602.
[44] X.D. Cong, R.J. Kirkpatrick, ^{29}Si MAS NMR study of the structure of calcium silicate hydrate, Adv. Cem. Based Mater. 3 (1996) 144–156.
[45] C.K. Lin, J.N. Chen, C.C. Li, NMR, XRD and EDS study of solidification/stabilisation of chromium with Portland cement and C_3S, J. Hazard. Mater. 56 (1997) 21–34.
[46] G.K. Sun, A.R. Brough, J.F. Young, ^{29}Si NMR study of the hydration of Ca_3SiO_5 and Ca_2SiO_4 in the presence of silica fume, J. Am. Ceram. Soc. 82 (1999) 3225–3230.
[47] M. Machida, R. Yamazaki, M. Aikawa, H. Tatsumoto, Role of minerals in carbonaceous adsorbents for removal of Pb(II) ions from aqueous solution, Sep. Purif. Technol. 46 (2005) 88–94.
[48] T. Vengris, R. Binkiene, A. Sveikauskaite, Nickel, copper and zinc removal from waste water by a modified clay sorbent, Appl. Clay Sci. 18 (2001) 183–190.
[49] A.K. Bhattacharyya, S.N. Mandal, S.K. Das, Adsorption of Zn(II) from aqueous solutions using different adsorbents, Chem. Eng. J. 123 (2006) 43–51.
[50] N.J. Coleman, D.S. Brassington, Synthesis of Al-substituted 11 Å tobermorite from newsprint recycling residue, Mater. Res. Bull. 38 (2003) 485–497.
[51] K.G. Bhattacharyya, S.S. Gupta, Adsorptive accumulation of Cd(II), Co(II), Cu(II), Pb(II), and Ni(II) from water on montmorillonite: Influence of acid activation, J. Colloid Interface Sci. 310 (2007) 411–424.
[52] C. Lu, H. Chiu, Adsorption of Zn(II) from water with purified carbon nanotubes, Chem. Eng. Sci. 61 (2006) 1138–1145.